Bogoliubov depletion of the fragmented condensate in the bosonic flux ladder

Andrey R. Kolovsky
Kirensky Institute of Physics, 660036 Krasnoyarsk, Russia
and Siberian Federal University, 660041 Krasnoyarsk, Russia
(Received 10 November 2016; published 20 March 2017)

We theoretically analyze the ground state of weakly interacting bosons in the flux ladder—the system that has been recently realized by means of ultracold atoms in the specially designed optical lattice [M. Atala, M. Aidelsburger, M. Lohse, J. T. Barreiro, B. Paredes, and I. Bloch, Nat. Phys. **10**, 588 (2014)]. It is argued that, for the system parameters corresponding to two degenerate minima in the Bloch dispersion relation, the ground state is a fragmented condensate. We study the Bogoliubov depletion of this condensate and discuss the role of boundary conditions.

DOI: 10.1103/PhysRevA.95.033622

I. INTRODUCTION

The possibility to mimic the bosonic flux ladder by using ultracold atoms in optical lattices, that was brought to reality in a laboratory experiment [1], has renewed the theoretical interest in this unordinary quantum system [2–7]. By definition, the ladder consists of two coupled one-dimensional (1D) lattices where the quantum particle hops along the ladder legs with the rate $J/\hbar$ and along the ladder rungs with the rate $J_\perp/\hbar$. The term "flux" means that the particle acquires a nonzero phase $2\pi\alpha$ when it encircles a plaquette of the ladder. For a charged particle this phase is introduced by a magnetic field perpendicular to the ladder plane. For a neutral atom one makes the hopping matrix elements complex by using nontrivial all-optical schemes—the approach known nowadays as artificial or synthetic magnetic fields [8–10].

One of the main features of the flux ladder is that the particle Bloch dispersion relation $E = E(\kappa)$ shows a bifurcation from that with two degenerate minima at $\kappa = \pm\pi\alpha$ to that with a single minimum at zero quasimomentum $\kappa = 0$ as the ratio $J_\perp/J$ is increased. This bifurcation has a number of consequences for observables. In particular, the time-of-flight images of cold atoms in the flux ladder have different numbers of peaks depending on inequality relation between $J_\perp$ and critical $J_\perp^* = J_\perp^*(\alpha)$, as it was well observed in the cited experiment [1].

The other, perhaps even more exciting, property of the system is that every Bloch state is a current-carrying state, with uniform currents flowing along the ladder legs in the opposite directions. We mention that the current is uniform only in the case of the periodic boundary condition. For other types of boundary conditions, like harmonic confinement or open boundaries, the current forms a vortex pattern with a single vortex for $J_\perp > J_\perp^*$ (one minimum in the Bloch dispersion relation) or several vortices for $J_\perp < J_\perp^*$ (two minima in the dispersion relation). This change in the vortex pattern has a remote analogy with the transition from Meissner's to Abrikosov's phase in a type-II superconductor [11], which is another reason explaining the large interest in the flux ladders.

Having observed a number of interesting effects already in the single-particle approximation, it is natural to ask the question about the role of atom-atom interactions which, within the Bose-Hubbard formalism, are characterized by the on-site interaction constant U. We recall that Bose particles in a 1D lattice with integer filling show a quantum phase transition in the parameter U/J from the superfluid phase to the Mott-insulating phase. In the past decade a lot of efforts were put towards obtaining the phase diagram of the bosonic flux ladder, and the new exotic phases, like the chiral Mott insulator, were theoretically predicted in the strongly interacting regime [3]. In the present work we focus on the opposite case of weakly interacting bosons. (The exact meaning of the term "weakly interacting" is given later in Sec. II C.) The particular problem we address is the structure of the many-body ground state of the system for $J_\perp < J_\perp^*$, where the single-particle Bloch dispersion relation has two degenerate minima at $\kappa = \pm q \approx \pm\pi\alpha$.

The addressed question is not trivial. In fact, let us denote by $\hat b^\dagger_{-q}$ and $\hat b^\dagger_{+q}$ the bosonic creation operators which create the particle in the Bloch states with $\kappa = \mp q$, respectively. Then there are at least three candidates for the ground state of weakly interacting bosons:

$$|\Psi\rangle \propto \frac{1}{\sqrt{2}}\left[e^{i\theta/2}\frac{1}{\sqrt{N!}}(\hat b^\dagger_{+q})^N + e^{-i\theta/2}\frac{1}{\sqrt{N!}}(\hat b^\dagger_{-q})^N\right]|\mathrm{vac}\rangle, \tag{1}$$

which is a superposition of two Bose-Einstein condensates with the relative phase θ;

$$|\Psi\rangle \propto \frac{1}{\sqrt{N!}}\left[\frac{1}{\sqrt{2}}(e^{i\theta/2}\hat b^\dagger_{+q} + e^{-i\theta/2}\hat b^\dagger_{-q})\right]^N|\mathrm{vac}\rangle, \tag{2}$$

which is a single condensate with broken translational symmetry; and

$$|\Psi\rangle \propto \frac{1}{(N/2)!}(\hat b^\dagger_{+q})^{N/2}(\hat b^\dagger_{-q})^{N/2}|\mathrm{vac}\rangle, \tag{3}$$

which is a fragmented condensate where $N/2$ particles occupy the Bloch state ψ_{-q} while the remaining $N/2$ particles occupy the Bloch state ψ_{+q}. We mention that Eq. (2) with proportionality sign substituted by the equality sign corresponds to the common single-orbital mean-field ansatz, where the exact value of the phase θ is then found by minimizing the energy functional. Notice that this ansatz explicitly breaks the translational symmetry of the system. On the contrary the multiorbital ansatz (3), which corresponds to the fragmented condensate, preserves the translational symmetry.

Clearly, any mean-field ansatz requires a justification, which implicitly assumes some microscopic analysis. This analysis may or may not confirm one's initial guess [12]. For example, it is argued in Ref. [13], which discusses a relevant problem of weakly interacting bosons in a square lattice with the uniaxial staggered flux, that the results of numerical diagonalization of the many-body Hamiltonian are consistent with the single-orbital mean-field ansatz (i.e., bosons do condense in a symmetry-broken state). Here we report a counterexample. It is shown below that the ground state of weakly interacting bosons in the flux ladder is of the form (3), where the proportionality sign denotes the leading term, which is followed by terms of smaller amplitude known as the quantum corrections to the mean-field solution. Going ahead we mention that these quantum corrections are responsible for the so-called Bogoliubov depletion of the condensate. We analyze the Bogoliubov depletion of the fragmented condensate and provide an analytical estimate for the number of depleted particles. In the work we also discuss the role of boundary conditions (BCs), the effect of which is particularly important for a moderate system size.

II. FLUX LADDER WITH PERIODIC BOUNDARY CONDITIONS

A. The model and single-particle spectrum

We begin with the case of periodic BCs where the last rung of the ladder is identified with the first rung. Labeling by (l,m) the individual sites of the ladder, the system Hamiltonian reads

$$\widehat{H} = \sum_{l=1}^{L}\sum_{m=1}^{2}\Big[-\frac{J}{2}(\hat{a}^{\dagger}_{l+1,m}\hat{a}_{l,m} + \text{H.c.}) - \frac{J_{\perp}}{2}(e^{i2\pi\alpha l}\hat{a}^{\dagger}_{l,m+1}\hat{a}_{l,m} + \text{H.c.}) + \frac{U}{2}\hat{n}_{l,m}(\hat{n}_{l,m}-1)\Big], \quad (4)$$

where $\hat{a}^{\dagger}_{l,m}$ and $\hat{a}_{l,m}$ are the creation and annihilation bosonic operators and $\hat{n}_{l,m} = \hat{a}^{\dagger}_{l,m}\hat{a}_{l,m}$ is the number operator. Notice that the Hamiltonian (4) conserves the total number of particles, which we denote by N. The elementary cell of the flux ladder (4) is determined by the Peierls phase α and for a rational $\alpha = r/p$ comprises p plaquettes. Following Ref. [1], we choose $J_{\perp}$ to be our control parameter and we measure this hopping matrix element and the interaction constant U in units of the hopping matrix element J (i.e., we set J to unity).

The first step of the analysis is to find the single-particle ($N = 1$) spectrum of the system. To obtain this spectrum it is convenient to change the gauge as follows:

$$\widehat{H} = \sum_{l=1}^{L}\sum_{m=1}^{2}\Big[-\frac{J}{2}(e^{i(-1)^m\pi\alpha}\hat{a}^{\dagger}_{l+1,m}\hat{a}_{l,m} + \text{H.c.}) - \frac{J_{\perp}}{2}(\hat{a}^{\dagger}_{l,m+1}\hat{a}_{l,m} + \text{H.c.})\Big]. \quad (5)$$

It is seen from Eq. (5) that for $J_{\perp} = 0$ the spectrum consists of two intersecting cosine dispersion relations which are shifted by $\pm\pi\alpha$ relative to $\kappa = 0$. Nonzero $J_{\perp}$ substitutes the band crossings at $\kappa = 0$ and $\kappa = \pm\pi$ by avoided crossings, thus resulting in the two-band spectrum $E = E^{(\pm)}(\kappa)$. An example is given in Fig. 1(a) for $\alpha = 1/3$ and $J_{\perp} = 0.5$, where locations of the energy minima are very close to $\kappa = \pm\pi/3$. As $J_{\perp}$ is increased, the minima move towards each other and eventually merge into the single minimum at $J_{\perp} = J^{*}_{\perp} \approx 2$. One finds a similar bifurcation of the energy spectrum for other α, excluding the case $\alpha = 1/2$ where positions of the minima are fixed at $\kappa = \pm\pi/2$.

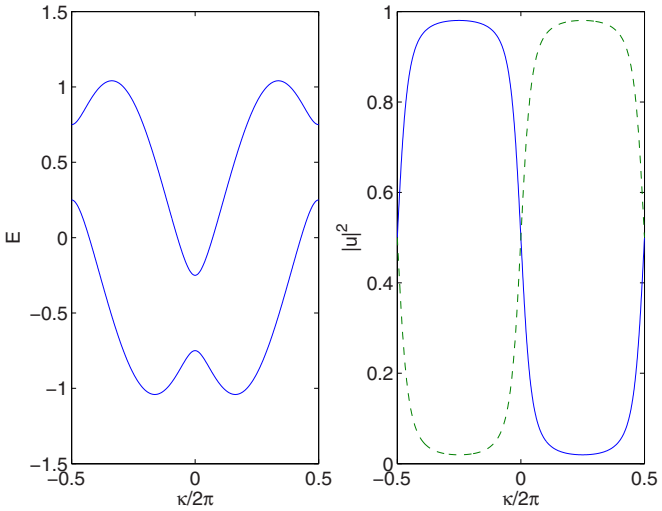

FIG. 1. Energy spectrum (dispersion relation) of a quantum particle in the flux ladder for $\alpha = 1/3$ and $J_{\perp} = 0.5$. The right-hand panel shows occupation of the ladder legs for a given Bloch state, where the dashed and solid lines refer to the lower and upper legs, respectively.

In addition to the dispersion relation we also need to know the explicit form of the Bloch states. Notice that, unlike the energy spectrum, the eigenstates do depend on the gauge. For the Hamiltonian (5) the Bloch states are given by

$$\psi^{(\pm)}_{l,m}(\kappa) = \frac{1}{\sqrt{L}}e^{i\kappa l}u^{(\pm)}_{m}(\kappa), \quad (6)$$

where $u^{(\pm)}_{1}(\kappa)$ and $u^{(\pm)}_{2}(\kappa)$ are probability amplitudes to find the particle in the lower and upper legs, respectively. For the purpose of future reference the right-hand panel in Fig. 1 shows squared amplitude u_m as the function of the quasimomentum κ for the ground Bloch band [minus sign in Eq. (6)]. It seen that for the quasimomentum κ around the energy minimum $\kappa = +q$ the quantum particle resides mainly in the upper leg, while for $\kappa = -q$ the situation is the inverse. This strong imbalance in the occupation of the ladder legs appears to be crucial for understanding the many-body spectrum of the system.

B. Many-body spectrum

We proceed with analysis of the many-body spectrum. Solid lines in Fig. 2 show the low-energy spectrum of $N = 4$ interacting bosons obtained by straightforward numerical diagonalization of Hamiltonian (1) for $\alpha = 1/3$, $L = 12$, with the periodic BC. Our prime interest in this figure is the lowest bunch of levels originating at $E/N = E_{\text{min}}$, where $E_{\text{min}} \approx -1.04$ is the single-particle energy of the ground. To analyze the depicted spectrum we use the approximation where one ignores the upper Bloch band. In other words, the field

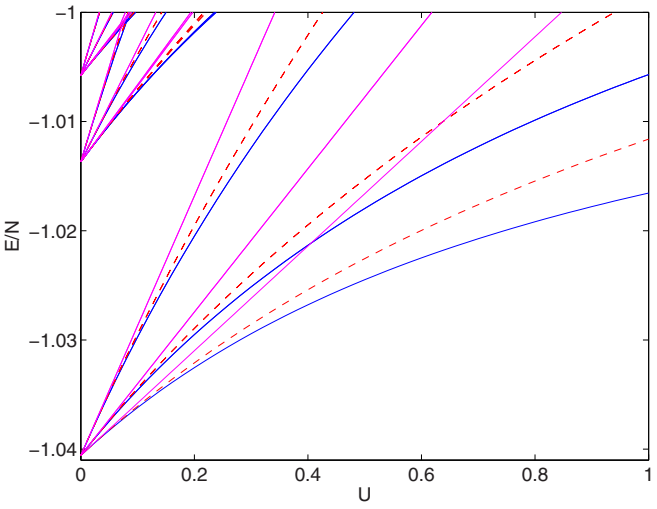

FIG. 2. Blue curves are the exact low-energy spectrum of $N = 4$ weakly interacting bosons in the flux ladder of length $L = 12$. The other parameters are the same as in Fig. 1. The dimension of the Hilbert space is $\mathcal{N} = 17\,550$. Dashed lines are the spectrum in the single-band approximation, where the dimension of the Hilbert space is reduced to $\mathcal{N} = 1365$. The straight magenta lines are the diagonal approximation (10), which ignores population of the other quasimomentum states besides $\kappa = \pm q$.

operator is given by $\widehat{\Psi}_{l,m} = \sum_\kappa \psi^{(-)}_{l,m}(\kappa)\hat{b}_\kappa$, where $\psi^{(-)}_{l,m}(\kappa)$ are the Bloch waves (6). Then the low-energy spectrum of the system (1) is determined by the Hamiltonian

$$\widetilde{H} = \sum_\kappa E(\kappa)\hat{b}^\dagger_\kappa \hat{b}_\kappa + \frac{U}{2L}\sum_{\kappa_1,\kappa_2,\kappa_3,\kappa_4} K(\kappa_1,\kappa_2,\kappa_3,\kappa_4) \times \hat{b}^\dagger_{\kappa_1}\hat{b}^\dagger_{\kappa_2}\hat{b}_{\kappa_3}\hat{b}_{\kappa_4}\delta(\kappa_1+\kappa_2-\kappa_3-\kappa_4), \quad (7)$$

where $E(\kappa) \equiv E^{(-)}(\kappa)$ is the dispersion relation for the lower band and the kernel

$$K(\kappa_1,\kappa_2,\kappa_3,\kappa_4) = \sum_{m=1}^{2} u^{(-)}_m(\kappa_1)u^{(-)}_m(\kappa_2)u^{(-)}_m(\kappa_3)u^{(-)}_m(\kappa_4). \quad (8)$$

The Hilbert space of Hamiltonian (7) is spanned by the quasimomentum Fock states $|\ldots,n_{-1},n_0,n_{+1},\ldots\rangle$, where n_{-1} is the number of particles in the Bloch state with the quasimomentum $\kappa = -2\pi/L$, n_0 is the number of particles in the zero-quasimomentum Bloch state, etc., and we place n_0 in the center of the Fock ket vector. The spectrum calculated by using Hamiltonian (7) is depicted in Fig. 2 by the dashed lines. A reasonable agreement is noticed. We mention, however, that the agreement becomes worse for larger U and the single-band Hamiltonian (7) is not suited, for example, to studying the quantum phase transition to the Mott-insulator state.

Next we employ the perturbation theory. Let us denote by $|\Psi_M\rangle$ the degenerate ground states of system (7) for $U = 0$,

$$|\Psi_M\rangle = |\ldots,0,N/2-M,0,\ldots,0,N/2+M,0\ldots\rangle, \quad |M| \leqslant N/2. \quad (9)$$

The states (9) obviously correspond to $2N+1$ possible distributions of N bosons between two energy minima. Infinitesimally small U removes the degeneracy where, according to the first-order perturbation theory, $E_M(U) = \langle\Psi_M|\widetilde{H}|\Psi_M\rangle$. After some algebra this gives

$$E_M(U) = E_{\min}N + \frac{U}{2L}[K_1(N^2/2+2M^2-N) + K_2(N^2-4M^2)], \quad (10)$$

where $K_1 = K(q,q,q,q)$ and $K_2 = K(q,-q,q,-q)$. The first term in the square brackets in Eq. (10) is the self-energy of state (9) due to virtual annihilation and creation of the particles in the same quasimomentum state [i.e., $\kappa_1 = \kappa_2 = \kappa_3 = \kappa_4$ in Eq. (7)]. The second term in the square brackets is a correction to the self-energy due to virtual annihilation and creation of the particles in the different quasimomentum states $\kappa = -q$ and $\kappa = +q$. Since the single-particle wave function $\psi_{l,m}(\kappa = \pm q)$ is essentially localized in one of two legs [see the right-hand panel in Fig. 1], we have $K_2 \ll K_1$. For example, for the considered ratio $J_\perp/J = 0.5$ the parameters $K_1 = 0.95$ and $K_2 = 0.05$.

The presented elementary analysis brings us to the first important conclusion. It follows from Eq. (10) that the lowest level in Fig. 2 has quantum number $M = 0$ and, hence, the state $|\Psi_0\rangle$, which is a fragmented condensate with $N/2$ particles occupying the quasimomentum state $\kappa = -q$ and the remaining $N/2$ particles occupying the state $\kappa = +q$, provides a zero-order approximation to the exact ground state. To find the latter analytically one should take into account the Bogoliubov depletion of the fragmented condensate $|\Psi_0\rangle$, i.e., nonzero occupations of the other quasimomentum states besides $\kappa = \pm q$. The Bogoliubov depletion is known to lower the system energy as compared to the diagonal approximation, and even a small depletion can cause considerable deviation from the linear law (10). In the next section we discuss the Bogoliubov depletion of the fragmented condensate in more detail.

C. Bogoliubov depletion of the fragmented condensate

There are two different approaches to the Bogoliubov depletion of Bose-Einstein condensates. The first approach (due to Bogoliubov) uses the substitution $\widehat{\Psi} = \Psi + \delta\widehat{\Psi}$ for the field operator $\widehat{\Psi}$, where Ψ is the mean-field solution. This approach results in the celebrated Bogoliubov–de Gennes equations, from which one finds both the quantum correction to the mean-field ground state and elementary excitations above the energy of the ground. Extension of the Bogoliubov–de Gennes theory to the case of fragmented condensates can be found in Ref. [14]. The second approach does not involve the mean-field solution and finds the ground state and the spectrum of elementary excitations directly from the microscopic Hamiltonian [15,16]. We follow the second approach, which was used earlier in Refs. [16,17] to study Bogoliubov depletion of ordinary condensates in the one-dimensional Bose-Hubbard system.

To find occupation probabilities of the other, besides $\kappa = \pm q$ quasimomentum states we use the ansatz

$$|\Psi\rangle = \sum_{n,k} c_{n,k}|\ldots,n,N/2-2n,n,\ldots,k,N/2-2k,k,\ldots\rangle. \quad (11)$$

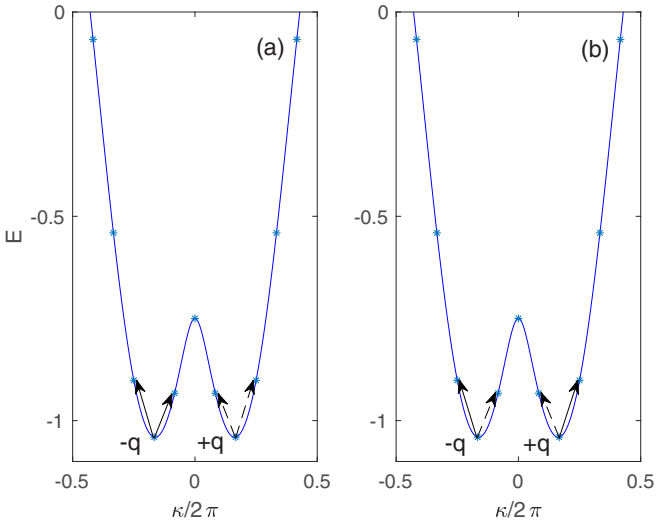

FIG. 3. Pictorial presentation of the Bogoliubov depletion. Two panels in the figure show two different kinds of the depletion processes which conserve the total quasimomentum of N particles. The example is given for $L = 12$ where discretization of the quasimomentum is $\Delta\kappa = \pi/6$.

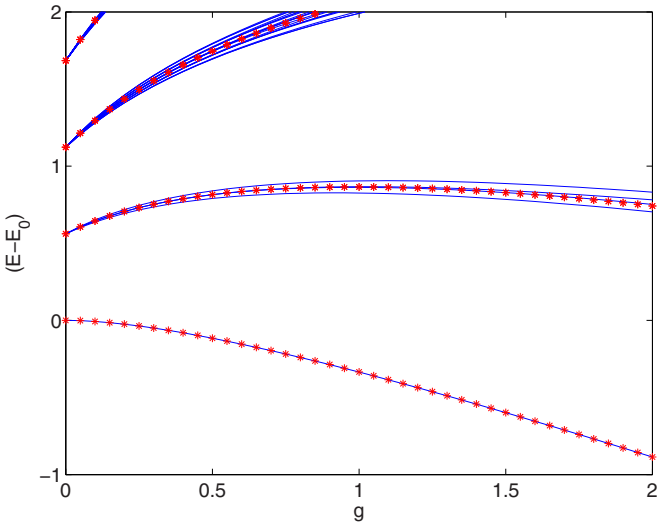

FIG. 4. Low-energy spectrum of system (7) as the function of the macroscopic interaction constant g. The other parameters are $N = 512$, $\alpha = 1/2$, and $L = 8$. The energy is measured with respect to mean-field energy E_0. Asterisks are the spectrum calculated by using ansatz (11).

Physically, the ansatz (11) corresponds to the process where one "takes" two particles from either of the condensates and puts them symmetrically (to satisfy the conservation law for the total quasimomentum) in the nearest quasimomentum states; see the left-hand panel in Fig. 3. Substituting Eq. (11) into the stationary Schrödinger equation with Hamiltonian (7) we obtain the following equation on the coefficients $c_{n,k}$:

$$E_0 c_{n,k} + \delta(n+k)c_{n,k} + \left(V_{n,k}^{(-q)} c_{n+1,k} + \text{H.c.}\right) + \left(V_{n,k}^{(+q)} c_{n,k+1} + \text{H.c.}\right) = E c_{n,k}, \tag{12}$$

where $E_0 = E_{\min} N + (U/2L)K_1(N^2/2 - N)$ is the energy of the not-depleted fragmented condensate and δ,

$$2\delta = E(\pm q - \Delta\kappa) + E(\pm q + \Delta\kappa) - 2E_{\min}, \tag{13}$$

is an increase in the kinetic energy due to population of the nearest quasimomentum states $\kappa = -q \pm \Delta\kappa$ and $\kappa = +q \pm \Delta\kappa$, $\Delta\kappa = 2\pi/L$.

Next we assume the semiclassical limit $N \to \infty$ and $U = gL/N \to 0$, where

$$g = NU/L \tag{14}$$

is the macroscopic interaction constant. In this limit the off-diagonal matrix elements $V_{n,k}^{(\pm q)}$ take a particular simple form, namely, $V_{n,k}^{(\pm q)} = K_1 g/2$. Furthermore, in the semiclassical limit Eq. (12) separates into two independent eigenvalue problems, so that $c_{n,k} = c_n c_k$. The corresponding equations for the coefficients c_n and c_k are identical and read

$$2(\delta + \tilde{g})nc_n + \tilde{g}(nc_{n+1} + \text{H.c.}) = (E - E_0)c_n,$$
$$E_0 \approx E_{\min} N + \tilde{g}N/4, \quad \tilde{g} = K_1 g/2. \tag{15}$$

Equation (15) can be solved analytically, resulting in the equidistant spectrum [16],

$$E_j = E_0 - (\delta + \tilde{g}) + \Omega(j + 1/2), \quad \Omega = 2\sqrt{2\tilde{g}\delta + \delta^2}. \tag{16}$$

For the purpose of future comparison, asterisks in Fig. 4 show the energy spectrum of system (7) calculated on the basis of Eq. (16) for the system parameters $N = 512$, $L = 8$, and $\alpha = 1/2$.

The approximation (16) for the low-energy spectrum can be improved further by taking into account the "correlated" depletion process, which corresponds to the following ansatz:

$$|\Psi\rangle = \sum_{n,k} c_{n,k} |\ldots, n, N/2 - n - k, k, \ldots,$$
$$k, N/2 - n - k, n, \ldots\rangle. \tag{17}$$

In other words, we take one particle from each condensate and distribute them symmetrically between the nearest quasimomentum states; see the right-hand panel in Fig. 3. We found that the depletion process (17) corrects Eq. (16) only slightly. Yet it removes degeneracy of the excited states E_j, where the level splitting is proportional to the parameter K_2; see solid lines in Fig. 4. Notice that, unlike in Fig. 2, in Fig. 4 we depict only the energy levels which correspond to zero total quasimomentum.

The presented results prove that, providing the condition $K_1 \gg K_2$, the Bogoliubov depletion of the fragmented condensate is similar to that of not-fragmented condensate. This allows us to obtain an analytical estimate for the number of depleted particles. Namely, knowing the eigenstates of Eq. (15), we calculate the depletion of each condensate as $N_d = \sum 2n|c_n|^2$. For the ground state of the original system this gives

$$N_d \approx 2\sqrt{\tilde{g}/\delta}, \quad \tilde{g} = K_1 g/2, \quad g = NU/L. \tag{18}$$

It follows from Eq. (18) that N_d diverges in the thermodynamic limit $N, L \to \infty$, where the parameter δ tends to zero as $\delta \sim 1/L^2$. This is in agreement with the well-known result that there could be no genuine condensate in an infinite 1D system.

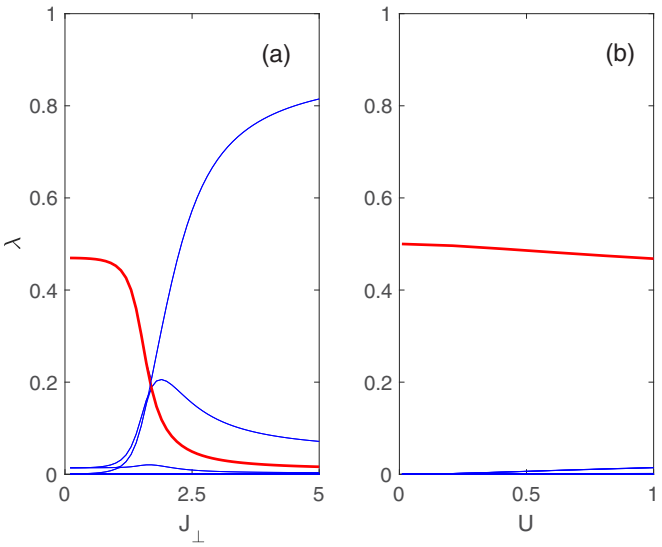

FIG. 5. Eigenvalues of the one-particle density matrix (19) (a) as the function of the hopping matrix element $J_\perp$ and (b) as the function of the interaction constant U. The other parameters are $N = 4, L = 12, \alpha = 1/3$, and (a) $U = 1$ and (b) $J_\perp = 0.5$. Notice that altogether we have 24 eigenvalues where the two degenerate largest eigenvalues, which are associated with the fragmented condensate, are depicted by the thick red lines.

Fortunately, in laboratory experiments with cold atoms one always deals with finite systems and, thus, N_d remains finite. Equation (18) also gives us the exact meaning of the term weakly interacting, namely, interactions are assumed to be weak if $N_d/N \ll 1$.

D. One-particle density matrix

The above-discussed depletion of the fragmented condensate can be easily detected by analyzing the one-particle density matrix,

$$\rho_{l,m}^{l',m'} = \frac{1}{N}\langle\Psi|\hat{a}_{l',m'}^{\dagger}\hat{a}_{l,m}|\Psi\rangle, \tag{19}$$

where $|\Psi\rangle$ is the ground state of system (4). Figure 5(b) shows eigenvalues λ_i of the matrix (19),

$$\rho_{l,m}^{l',m'} = \sum_{i=1}^{2L}\lambda_i\phi_{l',m'}^{*(i)}\phi_{l,m}^{(i)}, \tag{20}$$

as the function of the interaction constant U. It is seen that the density matrix has two degenerate eigenvalues close to $1/2$, which correspond to macroscopic occupations of the Bloch states with $\kappa = \pm q$. A decrease of these two largest eigenvalues as the interaction strength is increased indicates depletion of the fragmented condensate.

It is interesting to note that a system of rather small size can qualitatively reproduce the quantum phase transition associated with the bifurcation of the single-particle energy spectrum at $J_\perp = J_\perp^*$. Figure 5(a) shows eigenvalues of the density matrix as the function of $J_\perp$. It is seen in Fig. 5(a) that the fragmented condensate rapidly depletes as $J_\perp$ approaches the critical value $J_\perp^*$, and an ordinary condensate, where bosons condense in the Bloch state with zero quasimomentum, is formed for $J_\perp > J_\perp^*$.

To conclude this section we briefly comment on the time-of-flight (TOF) images of the fragmented condensate. In principle, the knowledge of the one-particle density matrix (20) suffices to predict TOF images of the expanding fragmented condensate. However, these predictions are valid only in the statistical sense. In the other words, the TOF images should be averaged over many runs of the same experiment. At a single run the TOF image is expected to be similar to that for not-fragmented condensate in the form (2), where one randomly peaks up the phase θ. This conclusion formally follows from the fact that the translationally invariant state (3) can be obtained from the symmetry-broken state (2) by averaging the latter over the phase θ [18]. With respect to some other systems the problem of how one can identify (and quantify) BEC fragmentation in a laboratory experiment is discussed in Refs. [21–23].

III. DIRICHLET BOUNDARY CONDITION

A. Single-particle ground states

As mentioned in the introduction, the Dirichlet BC (open boundaries) drastically changes the single-particle wave functions and, instead of uniform currents in the ladder legs, we get a vortex pattern for the persistent current. If $J_\perp > J_\perp^*$ there is only one vortex extending over the system size, while for $J_\perp < J_\perp^*$ there are several vortices with the characteristic size $\pi/|q|$. As before, we focus on the latter case, where the Bloch dispersion relation for the periodic BC would have two degenerate minima.

For the Dirichlet BC the new ground states of the system can be approximately expressed through the Bloch states (6) as

$$\tilde{\psi}_{l,m}^{(\pm)} = Y(l)\frac{1}{\sqrt{2}}[\psi_{l,m}(+q) \pm \psi_{l,m}(-q)], \tag{21}$$

where $Y(l) \approx L^{-1/2}\sin(\pi l/L)$ is a smooth envelope function. Examples of the symmetric (plus sign) and antisymmetric (minus sign) ground states are given by the dashed lines in Figs. 6(b) and 6(c) for $L = 12$ and in Fig. 8 for $L = 120$. Notice that, unlike the Bloch states for the periodic BC, the states (21) have equal population of the ladder legs, i.e., $|\tilde{\psi}_{l,1}|^2 = |\tilde{\psi}_{l,2}|^2$. Furthermore, the states (21) obey the reflection symmetry,

$$\tilde{\psi}_{l,1}^{(\pm)} = \pm\tilde{\psi}_{L-l+1,2}^{(\pm)}, \tag{22}$$

which we utilize later on. We mention, in passing, that one finds a similar symmetry also in the case of harmonic confinement, which is a more relevant BC from the viewpoint of a laboratory experiment with cold atoms. In this sense the BC considered in this section captures the physics of the realistic boundary conditions; however, it is simpler from the numerical viewpoint.

The other important result of the single-particle analysis is that the new ground states (21), which are locally given by symmetric and antisymmetric superpositions of the Bloch waves with the quasimomentum $\kappa = \pm q$, have slightly different energies. The energy difference $\Delta E = |E^{(-)} - E^{(+)}|$ between the symmetric and antisymmetric states can be very small, yet it remains finite. This is illustrated in Fig. 6(a), where

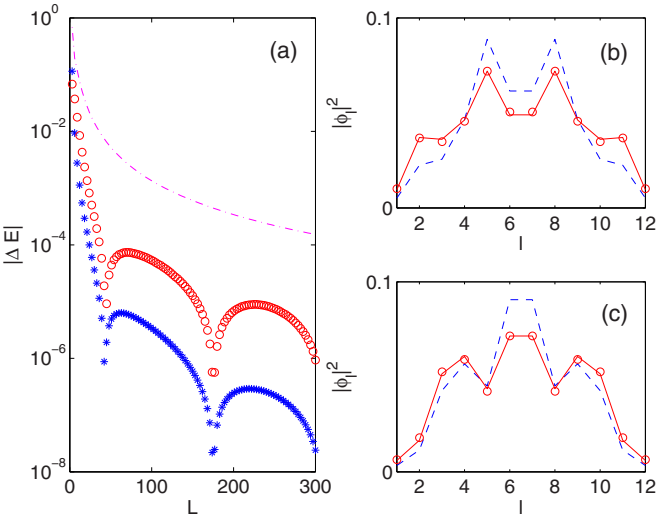

FIG. 6. (a) The energy difference $|\Delta E|$ between the two lowest eigenstates for $g = 0$ (asterisk) and $g = 1$ (open circles). The dashed line is the energy difference between the lowest duplet and the next eigenstate. The considered system size is $3 \leqslant L \leqslant 300$ with step $\Delta L = 3$. (b) Symmetric and (c) antisymmetric ground states for $N = 4$, $L = 12$, and $U = 0$ (dashed lines) and $U = 1$ (solid lines). Shown are the squared amplitudes $|\tilde{\psi}_{l,m}|^2$ and $|\phi_{l,m}|^2$, which are the same for $m = 1$ and $m = 2$.

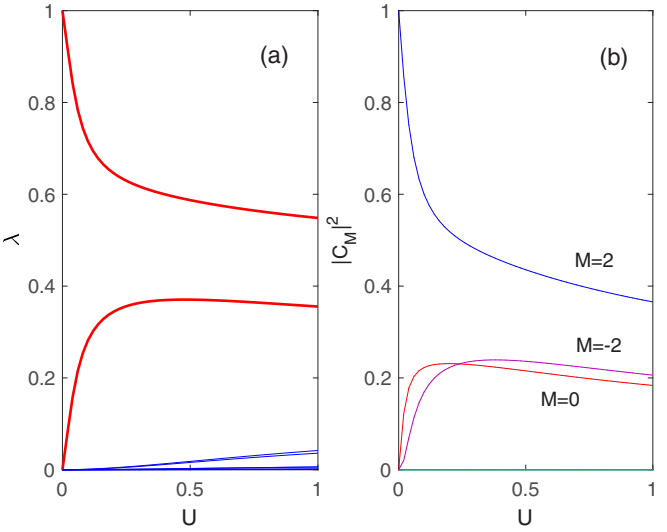

FIG. 7. (a) Eigenvalues of the one-particle density matrix (19) for the Dirichlet boundary condition. The two largest eigenvalues, which are associated with the symmetric and antisymmetric natural orbitals, are depicted by the thick red lines. (b) The overlap coefficients (24) as a function of the interaction constant U. The system parameters are the same as in Fig. 5(b) except for the different (Dirichlet) boundary condition.

we depict by asterisks the energy difference ΔE as a function of the system size L.

B. Many-body ground state

It follows from the previous section that for vanishing interparticle interactions the many-body ground state is an ordinary condensate, where bosons occupy the symmetric single-particle state. However, since the energy difference ΔE between the symmetric and antisymmetric states is rather small, one may expect that interactions force bosons to occupy both single-particle states. This conclusion is supported by the numerical analysis of the problem; see Fig. 7(a), which shows eigenvalues of the density matrix (19) as the functions of the interaction constant U. As U is increased, a considerable fraction of particles is seen to populate the antisymmetric state $\tilde{\psi}^{(-)}_{l,m}$, which has a slightly larger energy $E^{(-)} = E^{(+)} + 0.0011$. Additionally, the solid lines in Figs. 6(b) and 6(c) show the eigenvectors $\phi_{l,m}$ of the density matrix for the two largest eigenvalues, which should be compared with the single-particle states $\tilde{\psi}^{(\pm)}_{l,m}$ depicted by the dashed lines.

To obtain further information about the many-body ground state we project it onto the states $|\Psi_M\rangle$,

$$|\Psi_M\rangle = \frac{1}{\sqrt{(N/2+M)!(N/2-M)!}} (\tilde{b}^\dagger_+)^{N/2+M} (\tilde{b}^\dagger_-)^{N/2-M} |\mathrm{vac}\rangle, \tag{23}$$

where the operators $\tilde{b}^\dagger_\pm$ create the particle in the symmetric and antisymmetric single-particle states, respectively. The result is shown in Fig. 7(b), where we plot the squared modulus of the overlap coefficients,

$$C_M = \langle \Psi | \Psi_M \rangle. \tag{24}$$

It is seen in Fig. 7(b) that the exact ground state $|\Psi\rangle$ is a sum of three condensates, one fragmented [$M = 0$ in Eq. (23)] and two not fragmented ($M = \pm N/2$). Notice that strictly zero overlap coefficients $C_{\pm 1}$ prove that this state cannot be viewed as a single condensate, where bosons are condensed in some superposition of the symmetric and antisymmetric states.

The above-presented results suggest the following physical picture. For a large system size, where the energy difference ΔE between the symmetric and antisymmetric single-particle states is negligible, the ground state is the balanced fragmented condensate, similar to the case of periodic BC. As the system size is decreased, the energy difference ΔE increases and we have an admixture of not-fragmented condensates. We mention that one meets a similar effect in the problem of a single-mode spinor condensate subject to a magnetic field [12]. In both problems we have the energy difference between the single-particle states as an additional parameter. It is an open problem to find the overlap coefficients (24) as a function of the energy splitting ΔE or, which is essentially the same, as the function of the system size L.

C. Mean-field macroscopic wave functions

Finally, we analyze the macroscopic wave functions $\phi^{(\pm)}_{l,m}$ given by the first two eigenstates of the one-particle density matrix. We assume the large system size, so that the ground state of the system is a balanced fragmented condensate, and the weak interparticle interactions, so that the Bogoliubov depletion of this condensate is small. In this case we can find the functions $\phi^{(\pm)}_{l,m}$ by using the mean-field approach:

$$-\frac{J}{2}(\phi_{l+1,m} e^{-i\pi\alpha} + \phi_{l-1,m} e^{i\pi\alpha}) - \frac{J_\perp}{2}(\phi_{l,m+1}\delta_{m,1} + \phi_{l,m-1}\delta_{m,2}) + g|\phi_{l,m}|^2 \phi_{l,m} = E\phi_{l,m}, \tag{25}$$

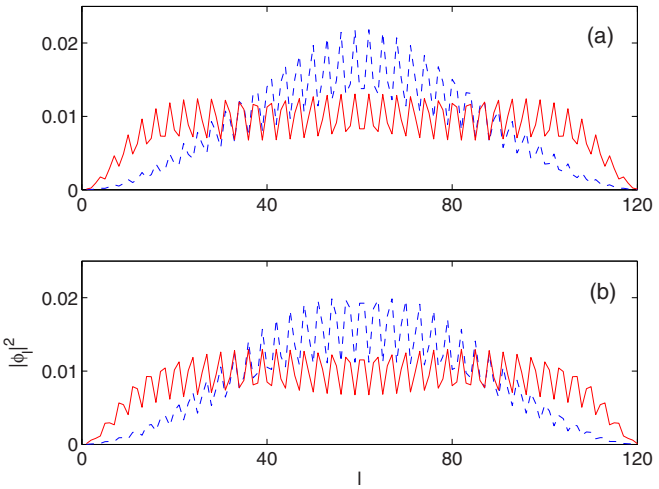

FIG. 8. Occupations $|\phi_{l,m}|^2$ of the ladder sites for $L = 120$ and $g = 0$ (dashed lines) and $g = 1$ (solid lines) for the (a) symmetric and (b) antisymmetric macroscopic wave functions.

where the macroscopic interaction constant g is defined in Eq. (14). Equation (25) is obtained by identifying the bosonic operators in Hamiltonian (5) with the classical canonical variables as $\hat{a}_{l,m}/\sqrt{N} \to \phi_{l,m}$ and $\hat{a}^\dagger_{l,m}/\sqrt{N} \to \phi^*_{l,m}$ [17]. The stationary nonlinear Schrödinger equation (25) can be simplified by noting that the ground single-particle states (21) possess the symmetry (22) and so do the eigenstates $\phi^{(\pm)}_{l,m}$ of the one-particle density matrix. Using this symmetry, Eq. (25) reduces to two one-dimensional problems,

$$-\frac{J}{2}(\phi_{l+1}e^{-i\pi\alpha} + \phi_{l-1}e^{i\pi\alpha}) \pm \frac{J_\perp}{2}\phi_{L-l+1} + 2g|\phi_l|^2\phi_l = E\phi_l, \qquad g = UN/L, \tag{26}$$

where the plus and minus signs refer to the symmetric and antisymmetric macroscopic wave functions, respectively. For $L = 120$ and $g = 1$ the minimal energy solutions of Eq. (26) are depicted in Fig. 8 by the solid lines. It is seen that repulsive interactions make the envelope function $Y(l)$ flatter, which is consistent with the role of interactions in the case of not-uniform wave functions. Yet, there are unremovable modulations of the particle density with the period $\pi/|q| \approx 3$, which are correlated with the vortex pattern for the persistent current. For the sake of completeness we also depict in Fig. 6(a) the difference ΔE between the mean-field energies of the symmetric and antisymmetric states.

It is interesting to note that, if we sum $|\phi^{(+)}_{l,m}|^2$ and $|\phi^{(-)}_{l,m}|^2$ with equal weights, the density becomes locally uniform. Keeping in mind that the uniform density minimizes the mean-field interaction energy, this result supports the above conclusion that in the limit of large L the ground state of the system is the balanced fragmented condensate.

IV. CONCLUSION

In the first part of the work we discussed the ground state of weakly interacting bosons in the flux ladder with periodic BCs, focusing on the case where the single-particle Bloch spectrum has two degenerate minima at $\kappa = \pm q$. It was shown that the many-body ground state is the fragmented condensate, where $N/2$ particles occupy the Bloch state with quasimomentum $\kappa = -q$ and the remaining $N/2$ particles occupy the Bloch state with quasimomentum $\kappa = +q$. We analyzed the Bogoliubov depletion of this fragmented condensate and obtained an analytical estimate for the number of depleted particles as the function of the interaction constant and the system size.

In the second part of the paper we addressed the case of Dirichlet BCs instead of the periodic BCs. The Dirichlet BCs explicitly break the translational symmetry of the system, so that the new nearly degenerate single-particle states show the vortex pattern for the persistent current. It was argued that, in the limit of large system size, the ground state of the system is again the fragmented condensate where the particles occupy the "symmetric" and "antisymmetric" macroscopic states. We calculated these macroscopic states by using a specific mean-field approach. This approach explicitly takes into account the fact that the ground state is a fragmented condensate and, in this sense, cardinally differs from the standard mean-field approach where the ground state is assumed to be an ordinary (not-fragmented) condensate.

Finally, we discuss the present work in the context of other works on fragmentation. Nowadays, fragmentation of Bose-Einstein condensates is a vast area of research [14,24–32], where Bose particles in the harmonic trap and in the double-well potential are the most popular systems. In this work we analyzed quite a different system, which can be viewed as an extension of the one-dimensional Bose-Hubbard model. Taking into account the importance of this model in cold-atom physics, the reported results contribute an interesting example of fragmentation in an *extended* system. We also emphasize that in the work our main approach was *microscopic* analysis of the many-body wave function, which does not appeal to a mean-field solution. It would be interesting to analyze the bosonic flux ladder by using the multiconfigurational mean-field theory [14,26]. This theory can give an accurate approximation to the exact many-body wave function by self-consistently finding the natural orbitals and their weights. Thus, in principle, it is capable of giving an answer to the above-posed question on the dependence of the expansion coefficients (24) on the system size L. We reserve this problem for future studies.

ACKNOWLEDGMENTS

The author acknowledges discussions with A. Eckardt, the hospitality of MPIPKS in Dresden, and financial support from Russian Foundation for Basic Research, Government of Krasnoyarsk Territory, and Krasnoyarsk Region Science and Technology Support Fund through Grant No. 16-42-240746.

[1] M. Atala, M. Aidelsburger, M. Lohse, J. T. Barreiro, B. Paredes, and I. Bloch, Observation of chiral currents with ultracold atoms in bosonic ladders, Nat. Phys. **10**, 588 (2014).

[2] M.-C. Cha and J.-G. Shin, Two peaks in the momentum distribution of bosons in a weakly frustrated two-leg optical ladder, Phys. Rev. A **83**, 055602 (2011).

[3] A. Dhar, M. Maji, T. Mishra, R. V. Pai, S. Mukerjee, and A. Paramekanti, Bose-Hubbard model in a strong effective magnetic field: Emergence of a chiral Mott insulator ground state, Phys. Rev. A **85**, 041602 (2012).

[4] D. Hügel and B. Paredes, Chiral ladders and the edges of quantum Hall insulators, Phys. Rev. A **89**, 023619 (2014).

[5] R. Wei and E. J. Mueller, Theory of bosons in two-leg ladders with large magnetic fields, Phys. Rev. A **89**, 063617 (2014).

[6] A. Tokuno and A. Georges, Ground states of a Bose-Hubbard ladder in an artificial magnetic field: Field-theoretical approach, New J. Phys. **16**, 073005 (2014).

[7] M. Piraud, F. Heidrich-Meisner, I. P. McCulloch, S. Greschner, T. Vekua, and U. Schollwöck, Vortex and Meissner phases of strongly interacting bosons on a two-leg ladder, Phys. Rev. B **91**, 140406(R) (2015).

[8] M. Aidelsburger, M. Atala, S. Nascimbene, S. Trotzky, Y. A. Chen, and I. Bloch, Experimental Realization of Strong Effective Magnetic Fields in an Optical Lattice, Phys. Rev. Lett. **107**, 255301 (2011).

[9] M. Aidelsburger, M. Atala, M. Lohse, J. T. Barreiro, B. Paredes, and I. Bloch, Realization of the Hofstadter Hamiltonian with Ultracold Atoms in Optical Lattices, Phys. Rev. Lett. **111**, 185301 (2013).

[10] H. Miyake, G. A. Siviloglou, C. J. Kennedy, W. C. Burton, and W. Ketterle, Realizing the Harper Hamiltonian with Laser-Assisted Tunneling in Optical Lattices, Phys. Rev. Lett. **111**, 185302 (2013).

[11] E. Orignac and T. Giamarchi, Meissner effect in a bosonic ladder, Phys. Rev. B **64**, 144515 (2001).

[12] E. J. Mueller, Tin-Lun Ho, M. Ueda, and G. Baym, Fragmentation of Bose-Einstein condensates, Phys. Rev. A **74**, 033612 (2006).

[13] G. Möller and N. R. Cooper, Condensed ground states of frustrated Bose-Hubbard models, Phys. Rev. A **82**, 063625 (2010).

[14] J. Grond, A. I. Streltsov, A. U. J. Lode, K. Sakmann, L. S. Cederbaum, and O. E. Alon, Excitation spectra of many-body systems by linear response: General theory and applications to trapped condensates, Phys. Rev. A **88**, 023606 (2013).

[15] A. J. Leggett, BEC in the alkali gases: Some fundamental concepts, Rev. Mod. Phys. **73**, 307 (2001).

[16] A. R. Kolovsky, Semiclassical Quantization of the Bogoliubov Spectrum, Phys. Rev. Lett. **99**, 020401 (2007).

[17] A. R. Kolovsky, Bose-Hubbard Hamiltonian: Quantum chaos approach, Int. J. Mod. Phys. B **30**, 1630009 (2016).

[18] A rigorous proof of the above statement would require a deeper insight into the measurement process, in the spirit of Ref. [19] aimed to explain the results of the fundamental experiment in Ref. [20] with fragmented Bose-Einstein condensate in a double-well potential.

[19] J. Javanainen and S. M. Yoo, Quantum Phase of a Bose-Einstein Condensate with an Arbitrary Number of Atoms, Phys. Rev. Lett. **76**, 161 (1996).

[20] M. R. Andrews, C. G. Townsend, H.-J. Miesner, D. S. Durfee, D. M. Kurn, and W. Ketterle, Observation of interference between two Bose condensates, Science **275**, 637 (1997).

[21] M.-K. Kang and U. R. Fischer, Revealing Single-Trap Condensate Fragmentation by Measuring Density-Density Correlations after Time of Flight, Phys. Rev. Lett. **113**, 140404 (2014).

[22] K. Sakmann and M. Kasevich, Single-shot simulations of dynamic quantum many-body systems, Nat. Phys. **12**, 451 (2016).

[23] A. U. J. Lode and Ch. Bruder, Fragmented Superradiance of a Bose-Einstein Condensate in an Optical Cavity, Phys. Rev. Lett. **118**, 013603 (2017).

[24] R. W. Spekkens and J. E. Sipe, Spatial fragmentation of a Bose-Einstein condensate in a double-well potential, Phys. Rev. A **59**, 3868 (1999).

[25] O. E. Alon and L. S. Cederbaum, Pathway from Condensation via Fragmentation to Fermionization of Cold Bosonic Systems, Phys. Rev. Lett. **95**, 140402 (2005).

[26] A. I. Streltsov, O. E. Alon, and L. S. Cederbaum, General variational many-body theory with complete self-consistency for trapped bosonic systems, Phys. Rev. A **73**, 063626 (2006).

[27] P. Bader and U. R. Fischer, Fragmented Many-Body Ground States for Scalar Bosons in a Single Trap, Phys. Rev. Lett. **103**, 060402 (2009).

[28] U. R. Fischer and P. Bader, Interacting trapped bosons yield fragmented condensate states in low dimensions, Phys. Rev. A **82**, 013607 (2010).

[29] U. R. Fischer, A. U. J. Lode, and B. Chatterjee, Condensate fragmentation as a sensitive measure of the quantum many-body behavior of bosons with long-range interactions, Phys. Rev. A **91**, 063621 (2015).

[30] M. C. Tsatsos and A. U. J. Lode, Resonances and dynamical fragmentation in a stirred Bose-Einstein condensate, J. Low Temp. Phys. **181**, 171 (2015).

[31] S. E. Weiner, M. C. Tsatsos, L. S. Cederbaum, and A. U. J. Lode, Phantom vortices: hidden angular momentum in ultracold dilute Bose-Einstein condensates, Sci. Rep. **7**, 40122 (2017).

[32] A. U. J. Lode, Multiconfigurational time-dependent Hartree method for bosons with internal degrees of freedom: Theory and composite fragmentation of multicomponent Bose-Einstein condensates, Phys. Rev. A **93**, 063601 (2016).